Doping of fullerite with molecular oxygen at low temperature and pressure

Yu. M. Shul´ga, V. M. Martynenko, A. F. Shestakov, S. A. Baskakov, S. V. Kulikov, V. N. Vasilets, T. L. Makarova, and Yu. G. Morozov*

Institute of Problems of Chemical Physics, Russian Academy of Sciences, 1 prosp. Akad. Semenova, 142432 Chernogolovka, Moscow Region, Russian Federation. Fax: +7 (496) 522 3670. E-mail: shulga@icp.ac.ru

Two methods are described for doping of fullerite C_{60} with molecular oxygen at a pressure of ~10^4 Pa and at temperature 20—30 °C. It was found by mass spectrometry using oxygen ^{18}O as dopant that a portion of molecular oxygen absorbed by the pre-decontaminated fullerite (first method) is removed as CO and CO_2 at the heating temperature ≤200 °C. Doping during fullerite precipitation from the liquid phase (second method) makes it possible to prepare samples with the oxygen content ≥1.2 at.%. The fullerite doped with oxygen to this level is diamagnetic. The paramagnetic properties of an O_2 molecule disappear when O_2 is incorporated into the fullerene lattice. This is interpreted on the basis of quantum chemical calculations as a sequence of equilibrium formation of the adduct $C_{60}O_2$. Calculations showed that the subsequent chemical transformation of $C_{60}O_2$ resulting in the O—O bond cleavage is energetically favorable, enabling prerequisites for the formation of products of incomplete (CO) and deep (CO_2) oxidation of fullerene under mild conditions.

Key words: fullerite C_{60}, intercalated with molecular oxygen, mass spectrometry, gasification on heating, magnetic properties, quantum chemical calculations.

It is known[1,2] that fullerite C_{60} with the face-centered cubic (fcc) lattice has one octopore (average radius R_{oh} = 2.06 Å) and two tetrapores (average radius R_{th} = 1.13 Å) per fullerene molecule. Atoms of some elements (Ar, Kr, and others)[3] and small molecules, *viz.*, CO,[4] CO_2,[5] and N_2O [6], can be located in these holes as "guests" in rather high concentrations without decomposition of the "host" lattice. Such a doping can sharply change the properties of fullerite. The appearance of superconductivity of compounds A_3C_{60} (A is an alkaline metal) with the fcc lattice is an example of the nontrivial result of such a doping (see, *e.g.*, review[7]). It was found[3,8] that the presence of atoms of inert gases in holes of the fullerite lattice affects the temperature of the phase transition fcc → SC (SC lattice is the simple cubic lattice) or changes the value of the pressure inducing this transition at room temperature. Filling of holes in fullerite can be considered as a convenient method for storage of rare gases, because filling of all octopores only (one gas molecule in each pore) corresponds to the volume concentration observed at a gas pressure of 5 MPa.[1]

At the same time, gas doping of solid fullerene resulting in filling of all its octopores requires high pressures and temperatures. For example, an inert gas pressure of 170—200 MPa and the temperature interval from 200 to 500 °C were used[3] to obtain compounds $Ar_{1.0}C_{60}$, $Kr_{0.9}C_{60}$, and $Xe_{0.66}C_{60}$. However, this method does not allow one to dope crystalline fullerite with reactive molecules, such as O_2. It was found[9] that a powder of the pure fullerite, which was stored in air, absorbed several percents of molecular oxygen. The ^{13}C NMR spectrum of this sample contains the main peak at δ 143.6 and a new peak at δ 144.3, whose appearance can be related[9] to the presence of paramagnetic oxygen molecules in the fullerite lattice. The appearance of the new peak in the ^{13}C NMR spectrum of the fullerite stored in air was confirmed in Ref. 10. It was also shown that heating of a sample *in vacuo* at 230 °C only decreases the intensity of the peak at δ 144.3. However, when air is used as an oxygen source, secondary phenomena are possible, because fullerite absorbs not only molecular oxygen but also N_2, CO, CO_2, Ar, and even H_2O.[11]

In this report, we describe two methods of fullerite doping with molecular oxygen and argon under mild conditions. Argon was chosen as dopant for comparison, because it can easily be identified. In our opinion, blocking of holes nearest to the crystallite surface with low-mobility atoms or molecules from the medium in which the crystalline fullerite was obtained or stored before experiment on doping is a reason why doping of the crystalline fullerite requires rigid conditions. Therefore, the first of the described methods includes the prolong pre-evacuation of a sample to be doped in high vacuum. The subsequent gas-phase doping was carried out at low tempera-

Published in Russian in *Izvestiya Akademii Nauk. Seriya Khimicheskaya,* No. 4, pp. 662—671, April, 2006.

1066-5285/06/5504-0687

ture and pressure. However, this method requires a long time and does not allow one to prepare samples with high content of a dopant.

The second method is to introduce a dopant at the step of lattice formation and makes it possible to obtain fullerite with a rather high content of a doping agent. The essence of the method is to create conditions for the introduction of a dopant into the fullerite lattice when the fullerite is precipitated from solution. Fullerenes can be precipitated from solution by two methods: (1) by evaporation of solvent and (2) by addition of a precipitating agent, *i.e.*, a substance that does not dissolve fullerene but is mixed with the solvent. In this work, we used for the preparation of fullerite the second method of precipitation, which can be performed at room or lower temperature. This method has been described earlier.[12,13]

In the present work, we also report new data on the physicochemical properties of the fullerite doped with molecular oxygen.

Experimental

Fullerite C_{60} with the fcc lattice (a_0 = 14.15 Å) and content of the main substance ≥99.5%, which was obtained by vacuum sublimation, was used as the initial sample. Before experiments on doping, the fullerite was evacuated at $2 \cdot 10^{-5}$ Pa for 2—3 days. The dopant gas was introduced at room temperature. The fullerite was stored under argon or oxygen ($9 \cdot 10^4$ Pa) for a period from 1 h to 3 days. The concentration of the absorbed gas increases with an increase in the storage time.

Experiments on doping during precipitation were carried out as follows. An unsaturated solution of fullerene (1 mg of C_{60} per mL of dichlorobenzene) was placed in a round-bottom flask, and argon or oxygen was purged through the solution. Then a fivefold amount (vol/vol based on the solvent) of isopropyl alcohol pre-saturated with the required gas was added. After the precipitating agent was added, the system was stored for 3—8 h in the dark. The solid phase that formed was filtered off. The solid phase was rlustrous dark crystals with the visible size down to 1 mm. Experiment was carried out, as a rule, at 0 °C. Before experiments on precipitation, the precipitating agent, *viz.*, isopropyl alcohol (IPA), was distilled over anhydrous potassium sulfate. The solvent, *viz.*, 1,2-dichlorobenzene (DCB), was purified with sulfuric acid and, after the acid was removed, distilled.

IR spectra of KBr pellets of the substance under study were recorded on a Perkin—Elmer Spectrum BX-II FTIR spectrometer. X-ray diffraction patterns were obtained using a DRON ADP-1 diffractometer (monochromatized Cu-Kα-radiation). Microanalysis was carried out by the microprobe method using a LEO-1450 scanning electron microscope (Carl Zeiss) equipped with an INCA Energy 300 attachment (Oxford Instruments). Magnetic properties were studied using a PARC M4500 vibrational magnetometer. ESR spectra in the 3-cm range were recorded on an SE/X-2544 spectrometer (Radiopan). Calorimetric measurements were performed on a DSC 822^e differential scanning calorimeter (Mettler Toledo) in the temperature interval from −40 to +200 °C with a heating rate of 10 deg min^{-1}. The chlorine concentration in samples was determined by the Schöniger method.[14]

Mass spectra of gases evolved by the solid phase on heating *in vacuo* were detected on an MI 1201V mass spectrometer. In this experiment, a weighed sample of the substance under study (400—500 mg) was placed in a quartz tube of the pyrolyzer, which was connected through a fine adjustment valve with the injection system of the mass spectrometer. The sample in the quartz tube was evacuated for 1 day to a pressure of ~$2 \cdot 10^{-5}$ Pa. This procedure is necessary to remove the surface and weakly bound impurities from the sample. After evacuation, the tube was isolated from the vacuum system, heated to a specified temperature T_1, and stored at this temperature for 3 h. Then the fine adjustment valve was open, and the gas collected in the tube at this heating stage was analyzed by mass spectrometry. Then the sample in the quartz tube at the temperature T_1 was evacuated again, and the valve was closed. The second collection of the gas phase was carried out at the temperature T_2 also for 3 h. These steps of analysis could be several, and $T_1 < T_2 < ... < T_n$. In typical experiments, $T_1 \approx 65$ °C, $T_2 < T_n < 400$ °C.

Results and Discussion

Doping according to the first method. The amount of the gas absorbed by the pre-deaerated fullerite increases slowly with time. Therefore, let us consider experimental results for the samples stored in the doping gas for 8 days to achieve maximum equilibration.

The peaks of the $[Ar]^+$ and $[Ar]^{2+}$ ions are most intense in the mass spectrum of argon used as dopant (Table 1). In the mass spectrum of the gases evolved from the argon-treated fullerite on heating to 65 °C, the peak with the maximum intensity also corresponds to the $[Ar]^+$ ion. The assignment of peaks with m/z = 44, 32, 20, 18, and 17 is doubtless: $[CO]_2^+$, $[O_2]^+$, $[Ar]^{2+}$, $[H_2O]^+$, and $[OH]^+$, respectively. As for the peak with m/z = 28, the $[N_2]^+$ and $[CO]^+$ ions can contribute to it, and the presence of the $[CO]^+$ ion is undoubtedly caused by the fragmentation of CO_2.

The mass spectrum of the gas phase evolved in the 65—100 °C temperature range differs sharply from the previous spectrum. The most intense was the peak with m/z = 32. The appearance of peaks with m/z = 32, 28, 16, and 14 in the spectrum implies, in our opinion, that the fullerite has absorbed N_2 and O_2 molecules on contact with oxygen before the experiment described. These molecules can be retained in the fullerite upon prolonged evacuation with heating to 65 °C. They occupy a part of fullerite pores thus preventing their filling with argon. Perhaps, pre-evacuation with heating should be carried out to increase the capacity of the fullerite with respect to argon. However, the heating should be slow and carried out to moderate temperatures to avoid the provocation of the chemical reaction with water or oxygen molecules until they are removed from the pores. In the experiment with argon, the main portion of the captured inert gas leaves the fullerite in the temperature interval ~20—65 °C.

Table 1. Mass spectra of argon (I) and gases isolated from the fullerite treated with argon (see text) upon its heating from ambient temperature to 65 °C (II) and from 65 to 100 °C (III)

m/z	I		II		III	
	I_{rel} (%)	Ion(s)	I_{rel} (%)	Ion(s)	I_{rel} (%)	Ion(s)
12	—	—	0.5	$[C]^+$	1.0	$[C]^+$
13	—	—	—	—	—	—
14	—	—	0.3	—	1.1	—
15	—	—	0.7	—	1.2	—
16	—	—	0.8	—	4.4	—
17	—	—	3.3	—	6.2	—
18	—	—	13.6	$[H_2O]^+$	24.5	$[H_2O]^+$
19	—	—	—	—	—	—
20	10.4	$[Ar]^{2+}$	9.3	$[Ar]^{2+}$	8.7	$[Ar]^{2+}$
21	—	—	—	—	—	—
25	—	—	—	—	—	—
26	—	—	1.5	—	2.0	—
27	—	—	7.2	—	8.6	—
28	—	—	8.7	$[N_2]^+$, $[CO]^+$	42.9	$[N_2]^+$, $[CO]^+$
29	—	—	0.8	—	1.2	—
30	—	—	—	—	0.5	—
31	—	—	0.3	—	0.3	—
32	—	—	6.3	$[O_2]^+$	100	$[O_2]^+$
33	—	—	—	—	—	—
39	—	—	—	—	—	—
40	100	$[Ar]^+$	100	$[Ar]^+$	65.8	$[Ar]^+$
41	—	—	0.7	—	1.1	—
42	—	—	0.5	—	0.6	—
43	—	—	1.5	—	2.1	—
44	—	—	3.2	$[CO_2]^+$	8.3	$[CO_2]^+$
45	—	—	—	—	—	—

If oxygen with the isotope composition $^{16}O : {}^{17}O : {}^{18}O = 0.10 : 0.12 : 0.78$ is used for doping instead of argon, then the gas phase above the sample at low temperatures (<100 °C) contains only oxygen sorbed by the fullerite at room temperature at the beginning of the experiment (Fig. 1). However, when heating the sample from 100 to 200 °C, the gas phase is enriched in CO and CO_2 (see Fig. 1, curve *4*). The appearance of peaks with $m/z = 30$ and 48 in the mass spectrum indicates that the gas phase contains CO and CO_2, which are the products of fullerene C_{60} oxidation with the heavy isotope ^{18}O. Thus, a portion of molecular oxygen absorbed by the fullerite is removed in the form of CO and CO_2 at the temperatures ≤200 °C. Note that the degree of doping according to the first method is rather low, so that the difference between the doped and undoped samples is not observed by IR spectroscopy and X-ray diffractometry.

Doping according to the second method. Fullerites prepared by precipitation from solution are comparatively new materials. The composition of these samples

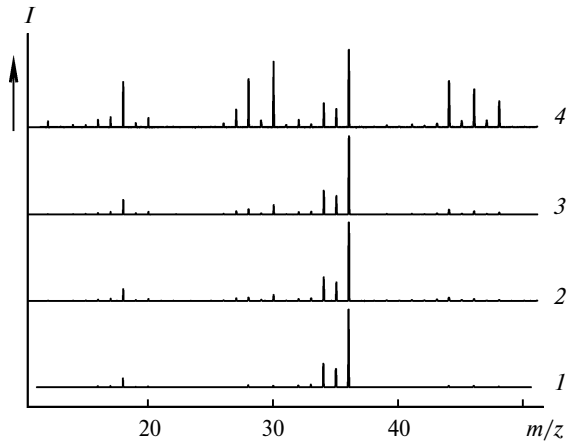

Fig. 1. Mass spectra of dioxygen enriched in the ^{18}O isotope used for doping of fullerite (*1*); gas phase above the fullerite doped with ^{18}O-enriched oxygen (*2*—*4*) after evacuation at $T = 20$ (*2*), 65 (*3*), and 100 °C (*4*) and $p = 9 \cdot 10^4$ Pa and subsequent heating from the ambient temperature to 65 °C (*2*), from 65 to 100 °C (*3*), and from 100 to 200 °C (*4*).

according to the microprobe analysis data (at.%) is given below.

Method of fullerite preparation	C	Cl	Ar	O
Precipitation from solution under Ar	99.11	0.22	0.04	0.63
Precipitation from solution under O_2	97.80	0.36	0.00	1.84

The samples consist mainly of carbon. The data presented on the argon content should be considered as a lower estimate, because the experimental conditions during analysis (vacuum, electron bombardment) result in intense argon desorption from the layer analyzed by the microprobe method. Oxygen is present in all the samples (even in the sublimate) due to specific features of the analytical procedure (oxygen is present in residual gases of the vacuum system). However, its content is much higher in the sample specially doped with oxygen. To estimate the oxygen content inside the oxygen-doped fullerite, one can, most likely, subtract the value determined for the argon-doped sample (0.63 at.%) from 1.84 at.% (see above). A comparison of the doping levels shows that for the described method of preparation the oxygen content is higher than the argon content by more than an order of magnitude.

The analysis data for the chlorine content should also be considered as a lower estimate, because, as shown below, the DCB molecules are evolved from the sample on heating.

The four most intense absorption bands (AB) in the IR spectra of both the initial fullerite and that prepared by precipitation (Fig. 2) coincide in position with the IR-active modes (F_{1u}) of the high-symmetry (I_h) C_{60} mol-

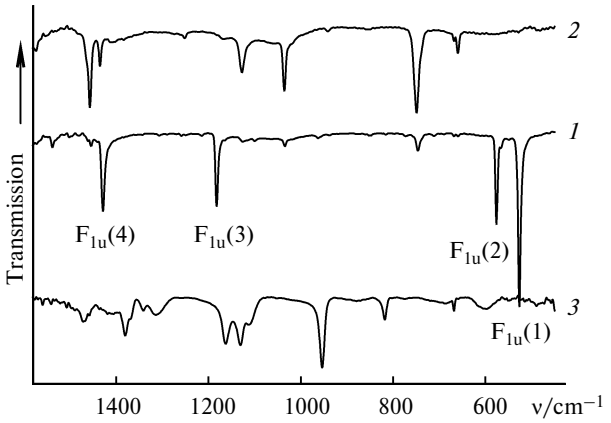

Fig. 2. IR spectra of the studied fullerite (*1*), dichlorobenzene (*2*), and isopropyl alcohol (*3*).

ecule (526.7, 576.2, 1182.7, and 1429.7 cm^{-1}).[15] The broad AB at 3437 and 1632 cm^{-1} (omitted in Fig. 2) are related to vibrations of the water molecules sorbed by a KBr powder (pellets were prepared in air). The DCB solvent appears in the IR spectra as several AB, most intense of which lying at 746.2 and 1034.4 cm^{-1}. The corresponding AB in the spectrum of the sample obtained by the addition of a DCB droplet to the potassium bromide powder appear at 749.2 and 1035.8 cm^{-1}. The spectrum of the fullerite under study also contains AB, which can be attributed to IPA (for instance, the AB at 955 cm^{-1}). Thus, it follows from the IR spectra that the fullerite precipitated from the liquid phase captures molecules of both the solvent and alcohol.

The X-ray diffraction patterns of the samples contain diffraction peaks caused by the fcc lattice of the fullerite (Fig. 3). For the fullerite prepared by precipitation, the intensity of the main peaks is the same as that for the initial fullerite. The crystallite sizes of the fcc phase in the samples under study (Table 2) in the direction perpendicular to the [*hkl*] plane were estimated by the Sherrer formula $D_{hkl} = \lambda/(\beta_{hkl}\cos\theta_{hkl})$ (λ is the wavelength of X-ray radiation, and β is the half-width of the diffraction peak). As can be seen from the data in Table 2, the crystallites of the fullerite prepared by precipitation are larger than those of the sublimate. Analysis of the shape of peak (111) showed that its asymmetry, which is expressed as a shoulder from the side of smaller angles, is most pronounced for the oxygen-doped fullerite, while it is least pronounced for the argon-doped fullerite. The sublimate occupies an intermediate position in this series. The appearance of this asymmetry and the peak marked with asterisk in Fig. 3 are related to distortions caused by the alternation of the main three-layer cubic and impurity two-layer hexagonal packings.[16]

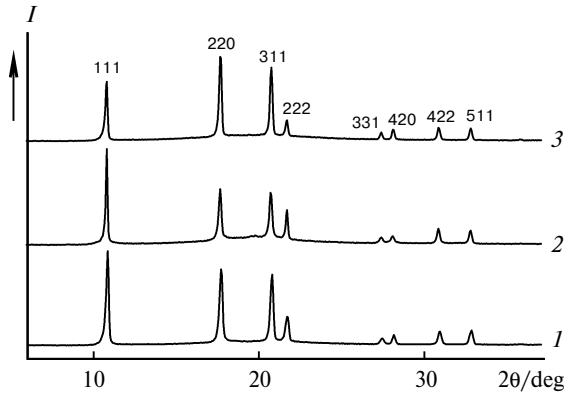

Fig. 3. X-ray diffraction patterns of the initial fullerite C_{60} (sublimate, *1*) and fullerites prepared by precipitation from a solution of fullerene in dichlorobenzene saturated with argon (*2*) and molecular oxygen (*3*).

Table 2. Parameters of the fcc lattice and crystallite sizes for the samples under study

Method of preparation of fullerite	a_0 /Å	D_{111}*	D_{220}
		nm	
Vacuum sublimation (initial)	14.15	96 (109)	87
Precipitation from solution under Ar	14.16	75 (99)	92
Precipitation from solution under O_2	14.21	142 (195)	96

* The D_{111} values obtained after subtraction of the contribution to the half-width of reflection 111 of distortions caused by impurities are given in parentheses (see text).

The fcc lattice constant for the doped samples exceeds that for the sublimate (see Table 2). This indicates unambiguously the presence of an impurity molecule in the lattice of the fullerite prepared by precipitation. Evidently, the DCB and IPA molecules cannot change the lattice parameters, since they cannot dope the fullerite because of the large size. The most probable candidates to this role are small molecules, such as H_2O, N_2, O_2, and carbon oxides (CO and CO_2), which, as known,[1–6] can occupy octopores of the fullerite, thus increasing the lattice parameter.

The mass spectra of the gas evolved from the fullerite, which was prepared by precipitation from argon-saturated solutions, are shown in Fig. 4. The heating stages are given in the figure caption. It is seen that the peak with $m/z = 28$ is most intense in spectrum *1*. This peak is attributed to the evolution from the sample of the nitrogen molecules, which were absorbed by the fullerite on its contact with air. The contact with air is also evidenced by the peak of oxygen with $m/z = 32$ and the value of the I_{32}/I_{28} ratio: it is the same as that in the mass spectrum of air. The peak with $m/z = 45$ is the second in intensity in spectrum *1*. This peak is caused by IPA, because the corresponding spectrum contains all peaks characteristic of IPA with approximately the same intensity ratio. The DCB

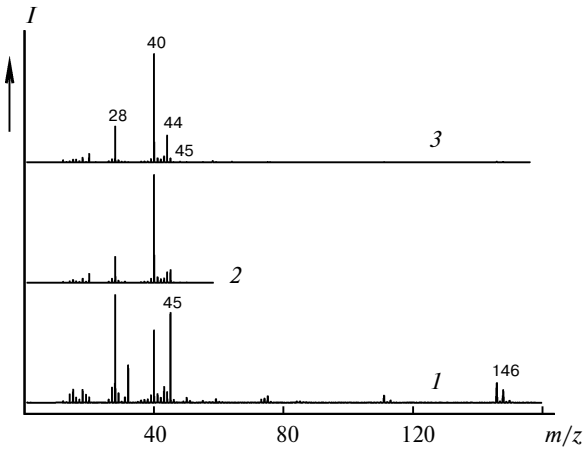

Fig. 4. Mass spectra of gases evolved from the fullerite, which was prepared by the precipitation of a solution of C_{60} in dichlorobenzene under argon on heating in the temperature intervals 17—100 (*1*), 100—200 (*2*), and 200—300 °C (*3*).

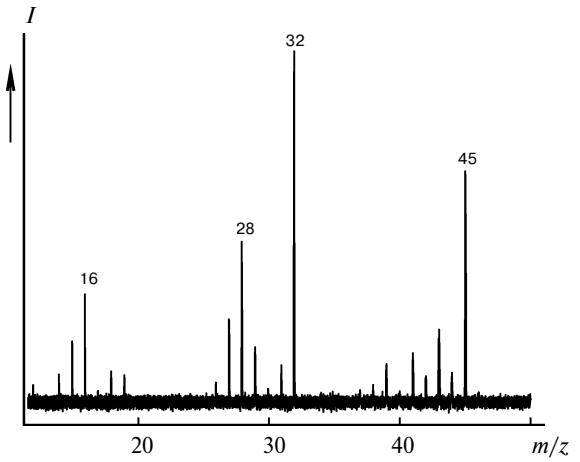

Fig. 5. Mass spectra of gases evolved from the fullerite, which was prepared by the precipitation of a solution of C_{60} in dichlorobenzene under oxygen on heating in the temperature interval from 60—100 °C.

solvent appears in the spectrum as a series of low-intensity peaks with m/z = 73, 74, 75, 111, 113, 146, 148, and 150. Among these peaks, the maximum intensity belongs to the molecular ion peak with m/z = 146. The peak of argon with m/z = 40 is only the third in intensity in the spectrum. In our opinion, this is related to the fact that argon in the near-surface layers of the fullerite particles is easily displaced by molecules of gases, which are present in air, on contact with air. Such an effect was not observed for the samples doped according to the first method, because no contact with air is implied by this method.

In the 100—200 °C temperature interval (see Fig. 4, curve *2*), argon becomes the main component of the gas above the fullerite. This is a sharp difference between the sample under study and the fullerite doped according to the first method for which the main portion of captured argon is evolved at temperatures <65 °C. Moreover, argon remains to be the main component of the evolved gas in the 200—300 °C temperature interval as well (see Fig. 4, curve *3*). This means, most likely, that the argon atoms in the samples under study lie in deeper layers, the escape from which requires a higher temperature.

An interesting fact is the high intensity of the peak with m/z = 28 (see Fig. 4, curve *3*). The nature of this peak changes during the temperature increase of the sample: in spectrum *1* this peak was caused mainly by the $[N_2]^+$ ions, while in spectrum *3* the $[CO]^+$ ions made the main contribution. The formation of carbon oxides is also confirmed by an increase in the intensity of the peak with m/z = 44 ($[CO_2]^+$ ions) and a decrease in the intensity of the peak with m/z = 14 ($[N]^+$ ions). It is seen that the fraction of IPA and DCB molecules decreases in the gas phase with the temperature increase.

Doping of the fullerite with oxygen results in the situation when at low temperatures oxygen is the main component of the gas mixture above the fullerite (Fig. 5). The peak with m/z = 28 is the second in intensity in spectrum *1*. This is related to the fact that on contact with air the near-surface fullerite layers actively absorb small molecules, in particular, N_2, which are constituents of air. When the temperature of the sample increases, the relative fraction of O_2 above the sample decreases but the fraction of carbon oxides increases.

Intercalation decreases the temperature of the phase transition (T_{pt}) fcc → SC (Table 3). The lower value of the specific heat of the transition (ΔH_{pt}) for the intercalated samples is caused, perhaps, by the presence of the amorphous part in their composition.

Magnetic properties. Fullerites C_{60} are known to be diamagnetics with low molar susceptibility χ_M. At room temperature (25 °C) the specific magnetic susceptibility ($\chi_{1/g}$) is $-0.35 \cdot 10^{-6}$ cm^3 g^{-1} and $\chi_M(C_{60}) = -252 \cdot 10^{-6}$ cm^3 mol^{-1}.[17,18] We obtained the value of $(-210 \pm 20) \cdot 10^{-6}$ cm^3 mol^{-1} for the fullerite prepared by the vacuum sublimation of the commercial sample. For the samples of the fullerite doped with molecular oxygen during low-temperature precipitation of solutions, the values found ranged from -70 to $-90 \cdot 10^{-6}$ cm^3 mol^{-1}. The accuracy of our measurements is $\pm 20 \cdot 10^{-6}$ cm^3 mol^{-1}.

At the same time, it is well known that an oxygen molecule in the ground state is paramagnetic. At room

Table 3. Results of DSC analysis of the fullerites under study

Method of preparation of fullerite	$-T_{pt}$ /°C	ΔH_{pt} /J g^{-1}
Vacuum sublimation (initial)	9.9	8.0
Precipitation from solution under Ar	18.2	5.7
Precipitation from solution under O_2	18.5	5.9

temperature the susceptibility χ_M for gaseous oxygen is[19] $+3440 \cdot 10^{-6}$ cm^3 mol^{-1}. Therefore, the presence of 0.00325 g of triplet oxygen in 1 g of fullerite is sufficient for the fullerite to become paramagnetic. Since the oxygen concentration is ≥1.2 at.% in the fullerite doped with O_2 during precipitation, retention of the diamagnetic properties of these samples indicates the absence of paramagnetic oxygen from them. This effect can be explained by different factors: (1) oxygen molecules form diamagnetic dimers, (2) strong exchange antiferromagnetic interaction appears between the oxygen molecules, and (3) diamagnetically bound state of C_{60} and O_2 is reversibly formed in the fullerite lattice. The formation of the $(O_2)_2$ dimers should be excluded, because their volume exceeds the volume of the fullerite pores. If the oxygen molecules are arranged one by one in the octapores of the fcc lattice of the fullerite as it has been found for other small molecules (see, *e.g.*, Ref. 20), then it is difficult to imagine that the antiferromagnetic interaction between them (J/k_B) would be >300 K, which is by an order of magnitude higher than the value for the α-phase of solid O_2 (30 K).[21] We believe that the formation of the oxygen—fullerene adduct in the octopore with rather strong chemical bonding, due to which the multiplicity of the C_{60}—O_2 system changes, is the most probable explanation of the effect observed.

Thus, the additional peak appeared in the ^{13}C NMR spectrum of the fullerite powder upon prolonged storage in air[9,10] cannot directly be attributed to the influence of paramagnetic O_2 molecules.

The sample under study is characterized by a very weak ESR signal with g = 2.0023 and a half-width of 0.11 mT at room temperature (Fig. 6). The concentration of spins resulting in this signal is $\sim 5 \cdot 10^{15}$ per g of the sample under study. Annealing of the sample *in vacuo* at 300 °C enhances the signal intensity by 13 times. The signal shape also somewhat changes. In the case of the argon-doped fullerite, the intensity and shape of the ESR signal are almost the same as those of the described signal. No annealing was carried out in the case of argon.

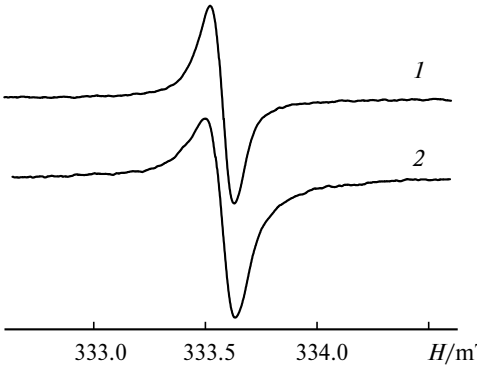

Fig. 6. ESR spectra of the fullerite doped with oxygen before (*1*) and after annealing *in vacuo* at 300 °C (*2*).

No ESR signal is expected for the ideal fcc lattice of the fullerite. The signal observed can be related to contaminations or structural imperfection of the lattice. The assumption on contaminations is most likely invalid, because earlier (see, *e.g.*, Refs 22 and 23), when fullerites of different quality and from different sources were used, the ESR signal parameters were similar to those obtained by us. According to published data,[23] the $[C_{60}]^+$ cations are structural imperfection resulting in the signal observed.

Note that the measured intensity of the ESR signal corresponds to the paramagnetic susceptibility $\chi_{1/g}$, being $\sim 10^{-4}$ at room temperature, which is substantially lower than the accuracy of our measurements of susceptibility.

Quantum chemical calculations. The disappearance of paramagnetism of the oxygen molecules when they get into the fullerite lattice along with the evolution of carbon oxides to the gas phase at rather low heating temperatures indicate the formation of any diamagnetic bound state of C_{60} and O_2. To reveal its nature, we performed quantum chemical calculations by the PBE density functional method[24] in the SBK basis set[25] using the PRIRODA program (see Ref. 26). The contribution of zero-point vibrations to the energy was taken into account in the harmonic approximation. When this level of the theory was used, the calculated fullerene structure (shortest C—C distances 1.402 and 1.454 Å) corresponds to the experimental electron diffraction data for the gas phase[27] (1.401(10) and 1.458(6) Å, respectively). In addition, the calculation in the same approximation of frequencies and intensities of IR vibrations for C_{60} gives good conformity with the experimental spectrum (Table 4).

The addition of O_2 to the C=C bond between two six-membered rings to form the dioxetane structure (Fig. 7) seemed most natural. In fact, as shown by the calculation, this structure is stable, and the energy of its formation from a singlet oxygen molecule and C_{60} is 37.1 kcal mol^{-1}. Taking into acount the experimental energy of singlet-triplet splitting in O_2 (Δ_{ST}) and the calculated statistical sums of C_{60}, $C_{60}O_2$, and O_2, one can estimate the free

Table 4. Experimental and calculated* frequencies (ν) and intensities (I) of $F_{1u}(n)$ vibrations in the IR spectrum of an C_{60} molecule (see Fig. 2)

n	ν/cm^{-1}		I_{theor} /km mol^{-1}	$I(n)/I(1)$	
	Experiment	Calculation		Calculation	Experiment**
1	526.7	524.5	70	1	1
2	576.2	576.4	40	0.57	0.52
3	1182.7	1182.4	27	0.39	0.41
4	1429.7	1450.5	38	0.54	0.44

* The calculation procedure is described in the text.

** The ratio of peak intensities in the experimental IR spectrum (KBr pellet).

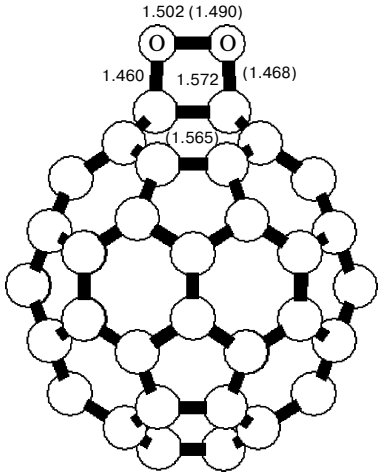

1a

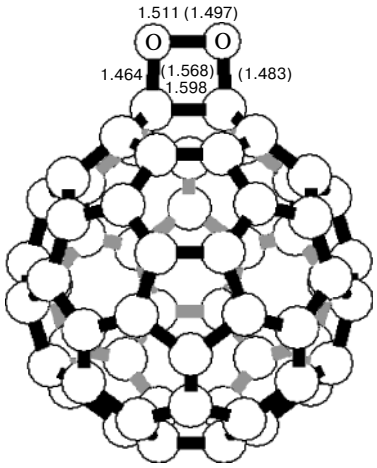

1b

Fig. 7. Structures of $C_{60}O_2$ projected on the symmetry plane (**1a**) and on the plane perpendicular to the symmetry plane (**1b**). Atoms and bonds behind the figure plane are gray-colored. Distances are given in Å. Values in parentheses concern the triplet state.

energy (ΔG) of $C_{60}O_2$ formation from an O_2 molecule in the ground triplet state as −3.2 kcal mol^{-1}. This semiempirical estimate seems more reliable than that obtained with the use of the directly calculated energy of formation resulting in the positive ΔG value. The reason is the overestimation of the Δ_{ST} value by 18 kcal mol^{-1} in the PBE/SBK approach. As known,[28] to obtain an adequate level of the singlet state of the oxygen molecule, one has to apply very wide basis sets along with sufficiently complete allowance for correlation effects. Therefore, taking into account the known similarity of the electronic structure of the O_2 fragment in the singlet $C_{60}O_2$ molecule and the singlet O_2 molecule, one can accept in the first approximation that errors in the calculated energies of O_2 and $C_{60}O_2$ are nearly the same. In essence, this is the only way to solve the problem, because it is almost impossible to calculate a rather large C_{60}—O_2 system at a level that would provide a sufficiently correct description of the energy position of the singlet level of the O_2 molecule.

Since the entropy of an oxygen molecule in the octahedral cavity of the fullerite is lower than that of a free oxygen molecule, the present calculation gives the free energy of $C_{60}O_2$ formation in the lattice exceeding −3.2 kcal mol^{-1}. It follows from this estimate that the fraction of paramagnetic oxygen in the lattice is low (but higher than 0.06%), which corresponds to our experimental data. The energy barrier to $C_{60}O_2$ formation is determined by the area of intersection of the triplet surface of the potential energy for the C_{60}—O_2 system and the singlet potential energy for the $C_{60}O_2$ adduct. Since the energy of the triplet state in the $C_{60}O_2$ adduct is higher than the energy of the singlet state by 27 kcal mol^{-1}, one should not expect high activation barriers in the approximation of linear intersection of the singlet and triplet terms (Fig. 8). The activation barrier for the related reaction of oxygen molecule elimination from fullerene ozonide was experimentally measured[29]: about 20 kcal mol^{-1}. Note that almost no spin density is observed on the oxygen atoms in the triplet $C_{60}O_2$ molecule. Therefore, in this case electrons are unpaired mainly in the carbon framework as in the C_{60} molecule and, hence, one should expect that this energy would be close to the energy of the triplet state in C_{60}, namely, 28.6 kcal mol^{-1}. This value is 34.6 kcal mol^{-1} when the contribution of zero-point vibrations is ignored. The energy of the vertical singlet–triplet transition is 37.6 kcal mol^{-1}, which is close to the value determined[30] by the B3lYP/6-31G* method: 36.9 kcal mol^{-1}. The experimental value of the energy of the 0—0 transition of a C_{60} molecule in the Xe matrix is 12714 cm^{-1}, *i.e.*, 36.3 kcal mol^{-1} (see Ref. 31).

In the calculated $C_{60}O_2$ structure **1a** (see Fig. 7), the O—O bond with a length of 1.502 Å is noticeably loosened compared to the triplet oxygen molecule (1.223 Å, experimental value 1.208 Å); the C—O and C—C bond lengths in the dioxetane cycle are 1.460 and 1.572 Å, respectively, and the length of the adjacent C—C bonds is 1.522 Å. For bonding an O_2 molecule, the frequency of the O—O vibrations also decreases noticeably from 1542 cm^{-1} (experimental value 1580 cm^{-1}) to 870 cm^{-1}. However, an insignificant intensity of this vibration (3.0 km mol^{-1}, effective mass 15.9) prevents its observation.

When searching for possible structures of $C_{60}O_2$, we found an unexpected variant of addition of an O_2 molecule to the C—C bond between the five-membered and six-membered rings **1b** (see Fig. 7). Its existence is caused, most likely, by the high extent of aromaticity of a fullerene molecule, despite nonequivalence of the C—C bonds. This state is higher in energy than the main isomer **1a** by only 15.8 kcal mol^{-1} and has a very close structure of the

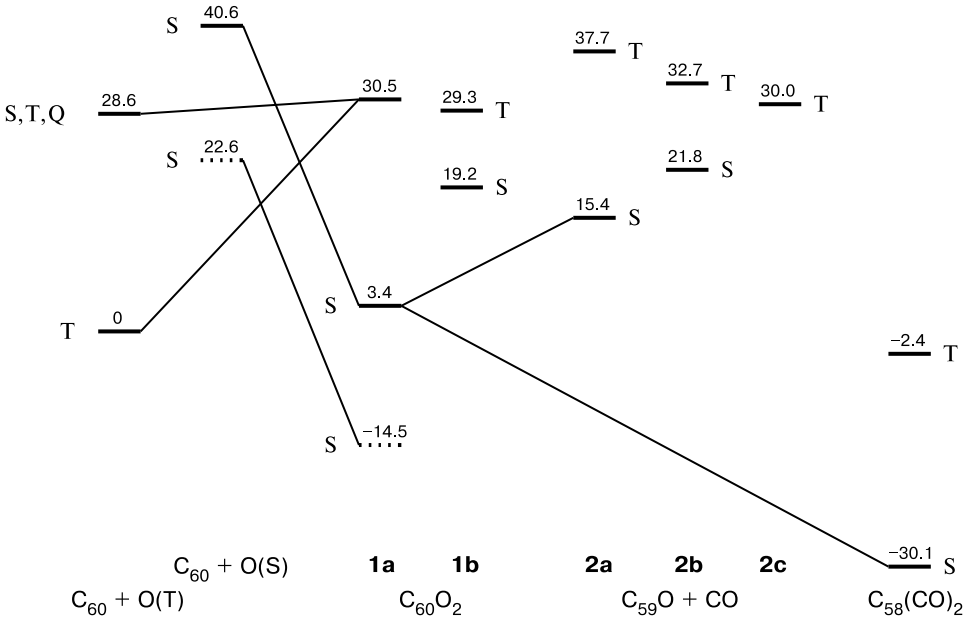

Fig. 8. Energy diagram from the adducts of C_{60} and O_2. The structures of isomeric forms are shown in Figs 7 and 9. Singlet, triplet, and quadruplet states are marked with letters S, T, and Q, respectively. Relative energies are given in kcal mol^{-1}. Dashed lines correspond to the levels obtained from the experimental value of singlet-triplet splitting in an oxygen molecule (see text).

dioxetane cycle: the O—O, O—C, and C—C bond lengths are 1.511, 1.464, and 1.598 Å, respectively. The lengths of the adjacent C—C bonds are 1.489 and 1.517 Å in the six- and five-angle cycles, respectively. The other C—C bond lengths in the C_{60} molecule change by at most 0.01 Å. The triplet state for this structure is also higher in energy, but the energy of singlet-triplet splitting is only 10.0 kcal mol^{-1} (see Fig. 8). It is by 1.2 kcal mol^{-1} lower than the triplet state of the isomeric structure and has another nature. More than a half of the spin density is concentrated in the belt of carbon atoms surrounding the C—C bond of the dioxetane cycle, and each oxygen atom has a spin density of 0.05.

The elimination of a CO molecule to form a sphere-like structure of $C_{59}O$ (**2a**) (Fig. 9) is endothermic with an energy effect of 18.3 kcal mol^{-1}. However, the isomeric form $C_{59}O$ (**2b**) containing the carbonyl group (see Fig. 9) is more stable (by 6.3 kcal mol^{-1}). In this case, among the three almost equivalent C—O bonds ~1.52 Å in length in structure **1a**, one bond is transformed into the short C=O bond (1.216 Å) and two other bonds are transformed into non-bonding C—O distances (3.133 Å) to the carbon

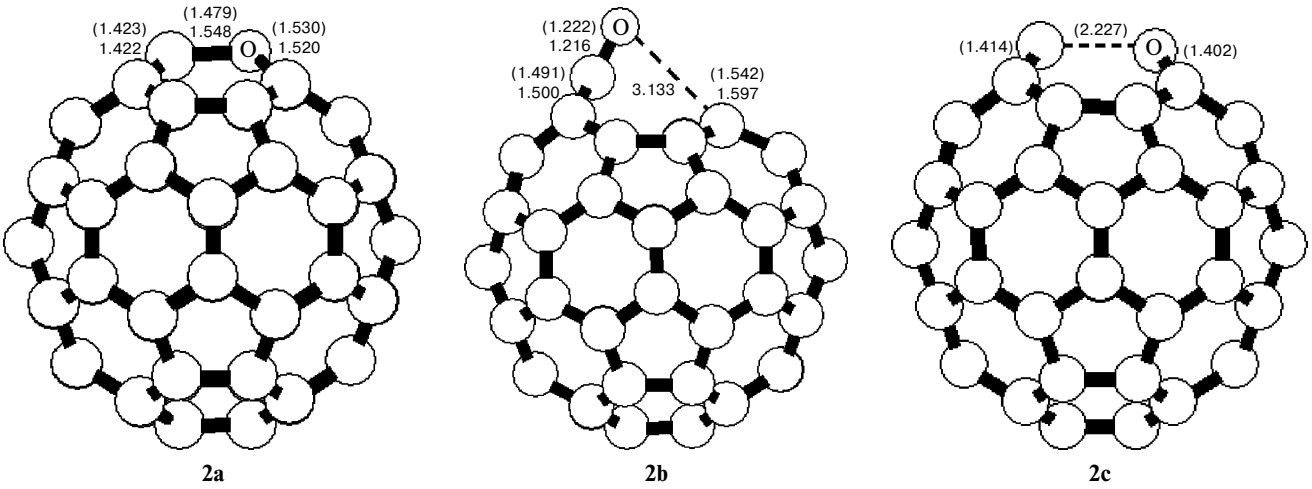

Fig. 9. Structures of $C_{59}O$ projected on the symmetry plane. Distances are given in Å. Values in parentheses concern the triplet state. Arrow indicates the C—C bond perpendicular to the figure plane.

atoms closing the four-membered ring after the cleavage of the C—O bonds. Just this structure mostly resembles the initial molecule $C_{60}O_2$ (see Fig. 6), and its formation in this process gives the change in the free energy almost equal to zero, taking into account an increase in entropy upon CO molecule liberation. The triplet states of these molecules are arranged more closely to the ground singlet state than in the case of the C_{60} molecule (see Fig. 8). Structure **2c** (see Fig. 9) with the nonplanar C_4O and C_5 cycles and a rather short non-bonding C...O distance of 2.227 Å has the lowest energy. The carbene C atom contains 60% of the spin density. An attempt to optimize this molecule in the singlet state results in the shortening of the C—O distance to form the earlier described structure with three C—O bonds. It is most likely that a rather strong donor-acceptor interaction involving the lone electron pair of the oxygen atom and the unoccupied p_σ-orbital of the C atom appears when the carbene fragment transits to the singlet state. According to the B3LYP/6-31G* calculation data,[31] the most stable $C_{59}O$ structure is that with the eight-membered carbon cycle, whose two bonds enter into the conjugated C_5 cycles. The energy of this structure is by 4.7 kcal mol^{-1} lower (ignoring the zero-point vibration energy) than the energy of the isomer with three C—O bonds. However, its formation needs the isomerization of the carbon skeleton.

The simultaneous cleavage of the O—O and C—C bonds in the $C_{60}O_2$ adduct results in the transformation of the latter into the structure with two carbonyl groups $C_{58}(CO)_2$ (Fig. 10). In this case, the energy gain is 33.6 kcal mol^{-1}, and the singlet-triplet splitting is almost the same as in the C_{60} molecule. The carbonyl groups cannot lie in the plane of the C_5 cycles because of steric hindrance. Two C=O groups shift considerably from the planes of the conjugated C_5 cycles and are arranged almost parallel to each other due to the distortion of the planar structure of the C_5 cycles and the shift of the C=O groups from the C_3 planes at the sp^3-C atoms with a deviation angle of 10.3°. In this case, a rather short (2.636 Å) O...O contact is formed. The repulsion between the oxygen atoms induces the extension of the parallel C—C bonds to 1.517 Å (inside the C_8 cycle framing the "hole" in fullerene). All these factors result in a noticeable strain of the nonplanar C_5 cycles $C_{58}(CO)_2$ and enhances their reactivity, for example, toward the oxygen molecule. Therefore, it can be assumed that the interaction of $C_{58}(CO)_2$ with O_2 in subsequent reactions of destruction of the carbon framework results in the formation of CO_2.

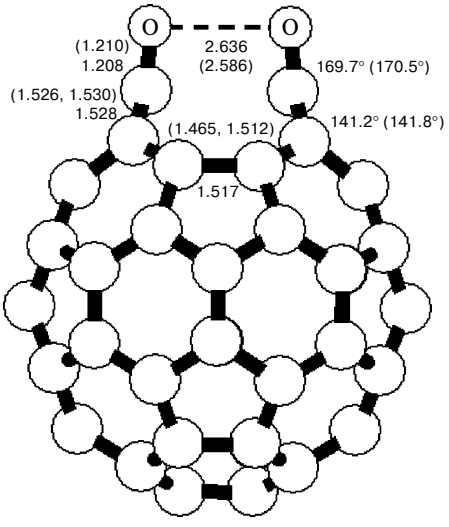

Fig. 10. Structure of $C_{58}(CO)_2$ projected on the symmetry plane. Distances are given in Å. Values in parentheses concern the triplet state. The presented angle values characterize the angle between the bond (CO) and plane and the angle between the planes inside the C_5 cycle. Two distances are given for the triplet state, because no exact mirror symmetry is observed.

Thus, the quantum chemical studies performed in this work allowed one to interpret the found disappearance of the paramagnetic properties of the O_2 molecule upon its entering into the fullerene lattice as follows. This phenomenon is caused by the equilibrium formation of the $C_{60}O_2$ adducts upon the primary interaction of fullerene C_{60} with molecule oxygen. The calculations show that the further chemical transformation of these adducts with the O—O bond cleavage are energetically favorable. This provides prerequisites for the formation of incomplete (CO) and deep (CO_2) oxidation products under mild conditions.

References

1. R. A. Assink, J. E. Shirber, D. A. Loy, B. Morosin, and G. Carlson, *J. Mater. Res.*, 1992, **7**, 2136.
2. M. J. Rosseinsky, *Mater. Chem.*, 1995, **5**, 1497.
3. G. E. Gadd, S. Moricca, S. J. Kennedy, M. M. Elcombe, P. J. Evans, M. Blackford, D. Cassidy, C. J. Howard, P. Prasad, J. V. Hanna, A. Burchwood, and D. Levy, *J. Phys. Chem. Solids*, 1997, **58**, 1823.
4. I. Holleman, G. von Helden, E. H. T. Olhof, P. J. M. van Bentum, R. Engeln, G. H. Nachtegaal, A. P. M. Kentgens, B. H. Meier, A. van der Avoird, and G. Meijer, *Phys. Rev. Lett.*, 1997, **79**, 1138.
5. G. E. Gadd, M. James, S. Moricca, D. Cassidy, P. J. Evans, B. Collins, and R. S. Armstrong, *J. Phys. Chem. Solids*, 1998, **59**, 1383.
6. M. James and G. E. Gadd, *Physica B*, 2000, **276—278**, 242.
7. L. Forro and L. Mihali, *Rep. Prog. Phys.*, 2001, **64**, 649.
8. J. E. Schirber, G. H. Kwei, J. D. Jorgensen, R. L. Hitterman, and B. Morosin, *Phys. Rev. B*, 1995, **15**, 12014.
9. R. A. Assink, J. E. Shirber, D. A. Loy, B. Morosin, and G. Carlson, in *Novel Forms of Carbon*, Eds C. L. Renschler, J. J. Pouch, and D. M. Cox, MRS Symposia Proceedings No 270, Pittsburgh, 1992, p. 225.
10. Z. Belahmer, P. Bernier, L. Firlej, J. M. Lambert, and M. Riber, *Phys. Rev. B*, 1993, **47**, 15980.

11. Yu. M. Shul´ga, V. M. Martynenko, S. A. Baskakov, and V. N. Fokin, *Zh. Fiz. Khim.*, 2004, **78**, 1725 [*Russ. J. Phys. Chem.*, 2004, **78** (Engl. Transl.)].
12. D. V. Schur, A. G. Dubovoi, N. S. Anikina, S. Yu. Zaginaichenko, V. D. Dobrovol´skij, V. K. Pishuk, B. P. Tarasov, Yu. M. Shul´ga, K. A. Meleshevich, A. P. Pomytkin, and A. D. Zolotarenko, *Proc. VII Intern. Conf. "Hydrogen Material Science and Chemistry of Metal Hydrides" (Alushta (Crimea, Ukraine), September 16—22, 2001)*, Alushta, 2001, 478.
13. Yu. M. Shul´ga, V. M. Martynenko, S. A. Baskakov, E. V. Skokan, I. V. Arkhangelskii, D. V. Schur, and A. P. Pomytkin, *Proc. VIII Intern. Conf. "Hydrogen Material Science and Chemistry of Metal Hydrides" (Sudak (Crimea, Ukraine), September 14—20, 2003)*, Sudak, 2003, 582.
14. W. Schöniger, *Mikrochim. Acta*, 1955, 123.
15. D. S. Bethune, G. Meijer, W. C. Tang, H. J. Rosen, W. G. Golden, H. Seki, C. A. Brown, and M. S. deVries, *Chem. Phys. Lett.*, 1991, **179**, 181.
16. E. V. Skokan, V. I. Privalov, I. V. Arkhangelskii, V. Ya. Davydov, and N. B. Tamm, *J. Phys. Chem.*, 1999, **103**, 2050.
17. R. S. Ruoff, D. Beach, J. Cuomo, T. McGuire, R. L. Whetten, and F. Diederich, *J. Chem. Phys.*, 1991, **95**, 3457.
18. A. P. Ramirez, R. C. Haddon, O. Zhou, R. M. Fleming, J. Zhang, S. M. McClure, and R. E. Smalley, *Science*, 1994, **265**, 84.
19. *Khimicheskaya entsiklopediya* [*Chemical Encyclopaedia*], Sovetskaya Entsiklopediya, Moscow, 1990, **2**, p. 387 (in Russian).
20. S. van Smaalen, R. Dinnebier, I. Holleman, G. von Helden, and G. Meijer, *Phys. Rev. B*, 1998, **57**, 6321.
21. C. Ueda, K. Sugiyama, and M. Date, *J. Phys. Soc. Jpn*, 1985, **54**, 1107.
22. M. D. Pace, T. C. Christidis, J. J. Yin, and J. Mailliken, *J. Phys. Chem.*, 1992, **96**, 6855.
23. S. K. Hoffman, W. Hilczer, W. Kempinski, and J. Stankowski, *Solid State Commun.*, 1995, **93**, 197.
24. J. P. Perdew, K. Burke, and M. Ernzerhof, *Phys. Rev. Lett.*, 1996, **77**, 3865.
25. H. Basch and P. G. Jasien, *Can. J. Chem.*, 1992, **70**, 612.
26. D. N. Laikov, *Chem. Phys. Lett.*, 1997, **281**, 151.
27. K. Hedberg, L. Hedberg, D. S. Bethune, C. A. Brown, H. C. Dorn, R. D. Johnson, and M. Devries, *Science*, 1991, **254**, 410.
28. P. Neogrady, M. Medved, I. Cernusak, and M. Urban, *Mol. Phys.*, 2002, **100**, 541.
29. D. Heymann, S. M. Bachilo, R. B. Weisman, F. Cataldo, R. H. Fokkens, N. M. M. Nibbering, R. D. Vis, and L. P. Chibante, *J. Am. Chem. Soc.*, 2000, **122**, 11473.
30. X. D. Li, W. D. Cheng, D. S. Wu, H. Zhang, Y. J. Gong, and Y. Z. Lan, *Chem. Phys. Lett.*, 2003, **380**, 480.
31. M. G. Giuffreda, F. Negri, and G. Orlandi, *J. Phys. Chem. A*, 2001, **105**, 9123.
32. H. Jiao, Z. Chen, A. Hirsch, and W. Thiel, *Phys. Chem., Chem. Phys.*, 2002, **4**, 4916.

Received September 22, 2005;
in revised form February 6, 2006